# Symmetry Considerations for the Targeted Assembly of Entropically Stabilized Colloidal Crystals *via* Voronoi Particles

Benjamin A. Schultz,[†] Pablo F. Damasceno,[‡] Michael Engel,[§] and Sharon C. Glotzer[*,†,‡,§,⊥]

[†]Department of Physics [‡]Applied Physics Program [§]Department of Chemical Engineering and [⊥]Department of Materials Science and Engineering, University of Michigan, Ann Arbor, Michigan 48109, United States

ABSTRACT The relationship between colloidal building blocks and their assemblies is an active field of research. As a strategy for targeting novel crystal structures, we examine the use of Voronoi particles, which are hard, space-filling particles in the shape of Voronoi cells of a target structure. Although Voronoi particles stabilize their target structure in the limit of high pressure by construction, the thermodynamic assembly of the same structure at moderate pressure, close to the onset of crystallization, is not guaranteed. Indeed, we find that a more symmetric crystal is

often preferred due to additional entropic contributions arising from configurational or occupational degeneracy. We characterize the assembly behavior of the Voronoi particles in terms of the symmetries of the building blocks as well as the symmetries of crystal structures and demonstrate how controlling the degeneracies through a modification of particle shape and field-directed assembly can significantly improve the assembly propensity.
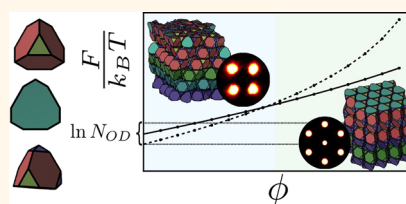
KEYWORDS: self-assembly · entropic forces · Monte Carlo simulation · hard particles · particle design

O nce a scientific curiosity, the assembly of nanoparticle superlattices and colloidal crystals is well on its way to becoming an industry. To attain such a status, however, requires that targeted crystal structures can be assembled with high quality and high yield from inexpensive, easy-to-make building blocks. Great strides in this direction have been achieved recently using DNA-programmable assembly.[1−4] At the same time, entropically stabilized superlattices of extraordinary complexity have been predicted[5−8] and, occasionally, observed by exploiting particle shape.[9−12] Although our understanding of the relationship between particle shape and crystal structure is quickly advancing, it is still not possible to predict *a priori* the crystals that will form from any arbitrary set of building blocks, nor the complementary prediction of the set of building blocks that will best assemble a given target structure. This latter challenge is the focus of the present paper.

As we will show, symmetry principles and entropic degeneracies play an important role for building block design. In atomic crystals, an empirical symmetry principle states that (i) the arrangement of atoms tends toward the highest possible symmetry, and (ii) counteracting factors due to special properties of the atoms may prevent attainment of the highest possible symmetry.[13] We argue that this principle should also apply for hard particles. Crystal structures of high symmetry are stabilized by entropy more frequently because they provide identical, more spherical local environments for each particle, thereby maximizing the average free volume per particle and, thus, the system entropy. For example, FCC and BCC are assembled by 41% of the polyhedra in Damasceno *et al.*[8] The "counteracting factors" that result in more complex structures come from pronounced shape anisotropies. Locally, however, entropy favors disorder and asymmetry, and in clusters, symmetry factors in the rotational partition function to destabilize highly symmetric clusters in favor of clusters of lower symmetry, as shown recently for clusters of micrometer-sized PMMA spheres.[14] This competition between local and global preferred symmetries makes building block design difficult.

Here we propose and test a design strategy based on the construction of particles whose shapes are given by the Voronoi tessellation of a target crystal structure, where the centers of the Voronoi cells represent the centers of the particles. These Voronoi particles (VPs) are space-filling and pack so that their centers reproduce the target structure. In particular, it can be shown that in the limit of high pressure, a densest packing necessarily becomes the thermodynamically favored structure. Thus, just like the construction of (often highly idealized) pair potentials guaranteed to produce the corresponding ideal crystal in the limit of zero temperature,[15,16] VPs are ideal shapes guaranteed to produce their target structure at high pressure. At intermediate pressure, however, VPs may assemble a thermodynamically stable or metastable crystals distinct from their target structure.[7] This means the packing problem (i.e., the search for the densest packing) and the assembly problem (i.e., the search for the crystal structure that assembles from the melt) have to be distinguished.[8,17−21]

Previous studies of the thermodynamics of space-filling shapes have been limited to the most symmetric polyhedra. In Agarwal et al.,[7] the melting (as opposed to assembly) behavior of six crystals of space-filling shapes was studied. In John et al.[22] the phase diagram of space filling tetragonal parallelepipeds was determined via melting simulations. Also, in Khadilkar et al.,[23] the assembly behavior of three different binary mixtures of binary space-filling polyhedra were studied, and it was reported that the space-filling crystals could be assembled only through the introduction of enthalpic patches. In this work, we investigate a large set of space-filling polyhedra in order to observe trends and correlations with particle shape. Our goal is to understand under which conditions VPs will assemble their target structure and to develop strategies for particle design based on our findings.

After introducing our model, we show that the majority (72%) of the VPs studied self-assemble an ordered structure. However, in fact only the simplest structures with the most symmetric VPs successfully assemble their space-filling target structures at moderate densities. To elucidate the role of particle symmetry and orientational entropic degeneracies, we identify metrics that correlate the assembly propensity of each target structure with aspects of particle shape. We then present a detailed study of the hexagonal diamond VP, which demonstrates how particle asymmetries can thermodynamically stabilize nonspace-filling structures due to orientational degeneracies. We comment on multicomponent VP systems, showing an example of an occupationally degenerate crystal. Finally, we leverage these results to devise two methods that are able to promote assembly of shapes otherwise notable to self-assemble their space-filling structure.
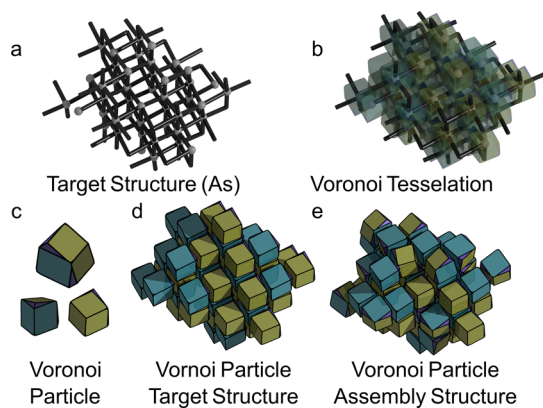
Figure 1. Construction and self-assembly of VPs: (a) an example target crystal (arsenic); (b) computed Voronoi tessellation; (c) VP from several views; (d) VPs in their space-filling target structure; (e) resulting equilibrium assembly from Monte Carlo simulation. Facets of the VPs are colored uniquely by shape.

VORONOI PARTICLE CONSTRUCTION AND PROPERTIES

The construction of Voronoi particles (VPs) via tessellation of target structures is performed as shown for the arsenic (As) crystal in Figure 1a−c. Starting with the target crystal structure, we compute the Voronoi tessellation, which divides space into a set of convex polyhedra, the VPs, by associating each point with the closest atom in the crystal. Each facet of the VPs corresponds to a nearest neighbor bond of the underlying crystal structure. In the figure, facets are colored by shape to highlight the types of bonds present. In a Voronoi tessellation, each VP facet is flush with an identical facet of a neighboring VP.

Following Damasceno et al.,[6] we characterize the roundness of a VP with the isoperimetric quotient $IQ = 36\pi V^2/A^3$, where V and A are the volume and surface area of the VP, respectively. Spheres have $IQ = 1$ and VP $0 \leq IQ < 1$. VP that tile space shapes are furthered constrained by a variant of the Kelvin conjecture (i.e., requiring cells of identical volume and shape) to $IQ < 0.7534$; the maximum is achieved in BCC.

A VP has the same point group symmetry as the Wyckoff position of the corresponding atom of the target structure. We quantify the symmetry of a VP by the order of its rotation group, N_{rot}, which contains elements of the point group with determinant one. The largest rotation group possible for a VP that tiles space is the O group of order 24. A VP can be further characterized by the distribution of its facet areas and shapes. We define $N_{f \geq \mu}$ to be the number of types of unique facets greater than or equal to the mean facet size and $N_{f,max}$ to be the multiplicity of the largest facet. Both quantities are positively correlated with N_{rot} but not entirely determined by it. For example, a 6-fold rotational axis may be centered in a hexagonal facet, or it may pass through a vertex about which six identical facets come together. It has been observed that large facets have the most significant impact for

TABLE 1. Table of VPs That Self-Assemble Their Space-Filling Structure

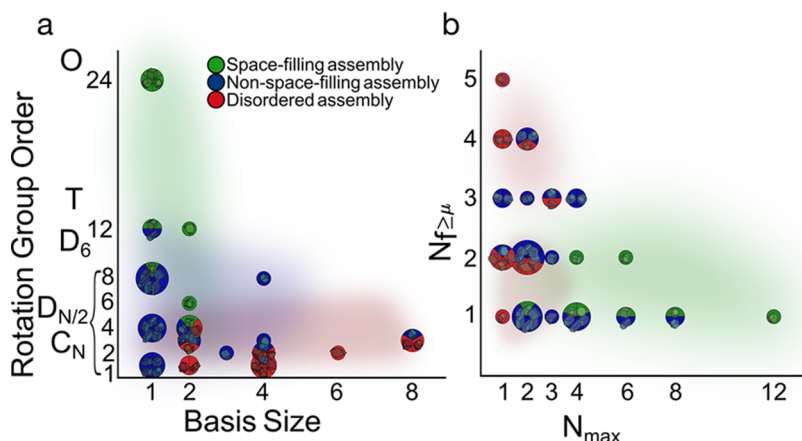| Number	Target Crystal	Image	Rotation Group	N_b	$N_{f \geq \mu}$	$N_{f,\max}$	IQ
1	BCC		O_h	1	1	8	0.7530
2	β-Sn		D_{2d}	2	2	4	0.6515
3	Cubic		O_h	1	1	6	0.5240
4	Diamond		T	2	1	4	0.4617
5	FCC		O_h	1	1	12	0.7400
6	HCP		D_{3h}	2	2	6	0.7405
7	Hexagonal, $a=1$, $c=1$		D_{6h}	1	1	2	0.6046
8	Tetragonal BC $a=b=1$, $c=2$		D_{4h}	1	1	4	0.6989

Figure 2. Summary of results from single VP assembly simulations. Green particles assemble their space filling structure (Table 1), blue particles form an ordered structure that is not the space-filling target structure (Supporting Information, Table SI-1), and red particles do not assemble an ordered structure on the time scales of our simulations (Table SI-2). (a) Assembly behavior as a function of the VP symmetry (rotation group order) and the complexity of the unit cell (basis size). (b) Assembly behavior as a function of the number of large facet types with area greater than or equal to the mean facet area, $N_{f \geq \mu}$, versus the multiplicity of the largest facet, $N_{f,\max}$.

assembly,[6,24] forming entropic "bonds"—emergent, effective attractions between particle facets. $N_{f \geq \mu}$ thus characterizes the types of misbonding that can occur between particles, while $N_{f,\max}$ characterizes the number of ways correct bonds can be established.
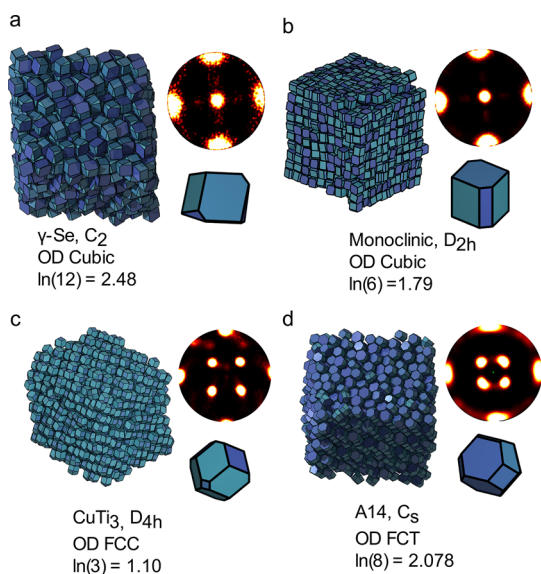
RESULTS

Single Voronoi Particle Assembly. We evaluate our strategy by selecting 46 atomic crystal structures[27] and Bravais lattices whose Voronoi tessellations contain a single Wyckoff position and thus yield a single type of particle shape. On the basis of their assembly behavior the VPs are grouped into three categories: VP that self-assembled into (i) their target structure (Table 1), (ii) an ordered structure that was not the

target structure (Supporting Information, Table SI-1), and (iii) no ordered structure on the time scale of our simulations (Table SI-2). Only the VPs of FCC, BCC, cubic, body-centered tetragonal, hexagonal, HCP, diamond, and β-Sn successfully assembled their target structure.

In Figure 2a, we show a scatter plot of the rotation group symmetry (N_{rot}) of the VP against the size of the crystal basis (N_B) that generated the VP. Because these metrics are discrete, several VPs map onto the same point; pie charts are drawn in these locations.

We observe that the highest symmetry VP (rotation group order $N_{rot} \geq 4$) corresponding to the simplest structures (basis size $N_B \leq 2$) are the most likely to assemble their space-filling structure. Degenerate,

a
γ-Se, C₂
OD Cubic
ln(12) = 2.48

b
Monoclinic, D₂ₕ
OD Cubic
ln(6) =1.79

c
CuTi₃, D₄ₕ
OD FCC
ln(3) = 1.10

d
A14, Cₛ
OD FCT
ln(8) = 2.078

Figure 3. Simulation snapshots of four VP systems that do not assemble space-filling structures but instead form orientationally degenerate (OD) structures. The assemblies show full positional order (characterized by bond order diagrams) but only partial orientational order. Under each snapshot, the name of the target structure is listed, followed by the point group of the VP. The second line lists the assembled crystal. The third line lists the entropy each particle contributes to the stabilization of the orientational degenerate structure relative to the space filling target structure.

dense local packings or bonded states (pairs of VPs with large aligned facets) that are incompatible with the assembly of space filling structures are a detriment to assembly propensity. The symmetry of the VP is anticorrelated with this quantity; the more symmetric the VP, the fewer unique ways it can arrange itself next to a neighbor.

As crystal structures become more complex, crystal symmetries are broken; this is reflected in the negative correlation between VP symmetry and the basis size. For crystal structures of moderate complexity, we find many VPs that assemble into structures other than their space filling target structures. VPs with very low symmetry, generated by crystal structures with the largest bases, tended to be poor assemblers; these VPs were the most "rock-like"[28] (*i.e.*, with low symmetry and many different types of large facets, $N_{f \geq \mu}$).

The majority of VPs self-assembled into orientationally degenerate, rather than space-filling structures. An orientationally degenerate diamond crystal (ODD) assembled by the hexagonal diamond VP is shown in Figure 4b). Additional examples are found in Figure 3: the VPs of γ-Se, monoclinic, CuTi₃, and A14 assemble 12-fold ($N_{OD} = 12$), 6-fold, 3-fold, and 8-fold orientationally degenerate crystals, respectively. Previously, the tetragonal parallelepiped (VP of the orthorhombic lattice) was reported to assemble into a 6-fold orientationally degenerate phase called a parquet phase.[22] Although the crystalline packing is argued from melting studies to be the thermodynamically preferred

state for parallelepipeds above $\phi_p \approx 0.7$,[22] we find only columnar and parquet phases to be accessible by assembly from the fluid phase for the aspect ratio we tested.

Previous work demonstrated that the assembly behavior of hard particles is influenced by shape parameters like the isoperimetric quotient, which quantifies the roundness of a particle, and the average coordination number of the dense fluid, which correlates with the number of large facets.[8] Recent work by van Anders *et al.*[24,29] quantifies the entropic valence associated with particle shape that explains the tendency for faceted particles to adopt face-to-face configurations, as observed in many studies.[5,6,8,30] For a VP to assemble its target structure, facets of the VP must bond selectively *via* entropy.

In Figure 2b), we examine assembly behavior as a function of $N_{f \geq \mu}$, the number of large facets, and $N_{f,\max}$, the multiplicity of the largest facet. Particles that successfully assemble their target structures typically have primarily only one type of large facet, and the VP has many copies of this largest facet. Particles with many types of facets (large $N_{f \geq \mu}$) suffer from non-selectivity of entropic bonds. Some particles with several such facets (higher symmetry, large $N_{f,\max}$) still crystallize, while particles with too many competing facets (large $N_{f \geq \mu}$) with low multiplicity (small $N_{f,\max}$) are poor assemblers.

An Example: Hexagonal Diamond Voronoi Particle. The results of the previous section demonstrate that orientational degeneracy is capable of stabilizing nonspace-filling crystals (blue in Figure 2). As a representative example for this behavior, we consider the VP for hexagonal diamond (HD, Wurzite). This VP (Figure 4a) is a truncated tetrahedron with three augmented tips and thus has a 3-fold rotation axis (point group (C_{3v}). There are two large facet types (red, cyan). In the target structure (Figure 4c), red facets are adjacent to one another and cyan facets are adjacent to one another. Yet, at the onset of order ($\phi_p = 0.59$), we did not observe the selective red—red, cyan—cyan bonding of the HD structure. Instead, the VPs assembled a 4-fold orientationally degenerate diamond crystal (ODD), where the VPs bond nonselectively (Figure 4b).

It can be shown that the ODD is related to HD exactly as FCC is related to HCP and both structures exhibit tetrahedral coordination. Thus, we expect their free energies to be nearly identical and the ODD to be stabilized solely by the entropy associated with the orientational degeneracy. Our calculations confirm this: the ODD has lower free energy than HD up to $\phi_p = 0.77$ (Figure 4d). The preference of ODD over HD just above the onset of order, $\phi_p = 0.59$, can also be confirmed directly in fluid—solid coexistence simulations (see Supporting Information). However, we are unable to observe the crossover at $\phi_p = 0.77$, because at these high densities the simulations become
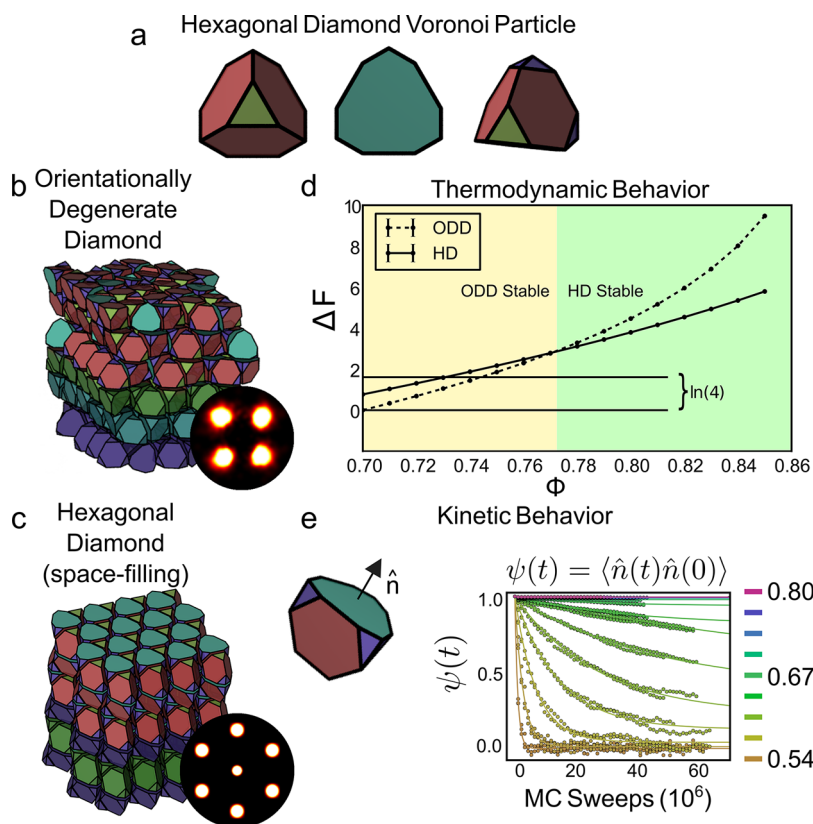
Figure 4. (a) HD VP from several views. (b) Assembly structure of the HD VP, the ODD structure. This structure is composed of tetrahedrally closed packed layers in which the HD VP adopt one of four equivalent orientations (top three layers), and stack ABC (bottom three layers). (c) Space-filling target structure of the HD VP. The particles have no orientational degeneracy (top three layers) and stack AB (bottom three layers). (d) Free energy difference between these two structures. The orientational degeneracy stabilizes the nonspace filling structure up to the density $\phi_p = 0.77$. (e) Orientational correlation function near the predicted thermodynamic transition for different values of ϕ_p. The HD VP is kinetically arrested before the thermodynamic ODD to HD phase transition.

nonergodic. Examination of the rotational dynamics of the HD VP near crossover demonstrates nonergodicity (Figure 4e). The rotational autocorrelation function $\psi(t) = \langle \hat{n}(t)\hat{n}(0) \rangle$, where $\hat{n}(t)$ is a particle director, does not decay on the time-scale of our simulation.

To get an impression for the magnitude of the thermodynamic driving force for crystallization into orientationally degenerate versus nondegenerate crystals, we note that in van Anders et al.,[24] the potential of mean force and torque (PMFT) calculated for comparably truncated tetrahedra produces entropic bond strengths in the ODD of $\sim 2.5 k_B T$. Thus, the entropic forces driving the assembly of the ODD relative to HD, $\ln(4)k_B T = 1.4 k_B T$ are comparable to the emergent forces driving crystallization quantified by the PMFT. To stabilize HD over ODD at lower packing fractions would require additional interparticle interactions, as in Khadlikar et al.,[23] and the magnitude of the required interactions must overcome the entropy from orientational degeneracies.

Beyond Single Component Systems. Many crystals have two (or more) Wyckoff positions and thus generate two (or more) VPs. Binary mixtures of hard particles may crystallize,[31,32] or phase separate.[33] We studied a limited set of two-VP target structures to provide examples of VP phase behavior unique to multicomponent VP systems. We did not observe any shape mixtures that crystallized into their space-filling structure. Instead, we observed phase separation (in VPs of the PtS crystal), mixtures that did not crystallize on the time scale of our simulation, and several examples that crystallized into a binary nonspace-filling crystal.

The VPs generated by the trigonal-ω crystal (Figure 5 a–g) crystallize into an orientationally degenerate, nonspace-filling BCC crystal, in which the type of VP at each lattice site is random. This occupational degeneracy creates mixing entropy, which can be thought of in the same manner as orientational degeneracy for single-component systems. To first order (neglecting differences in rattling free volumes for each component), the mixing entropy for a binary mixture of species fraction of f and $1 - f$ has an identical form to that of the mixing entropy of a lattice gas, $F_{\text{mixing}}/N = k_B T(f \ln f + (1 - f) \ln(1 - f))$. For trigonal-$\omega$ we have $f = 2/3$, which gives a contribution of $0.64 k_B T$ toward stabilizing the occupationally degenerate crystal relative to the space-filling target structure. We only observed occupational degeneracy in crystals with
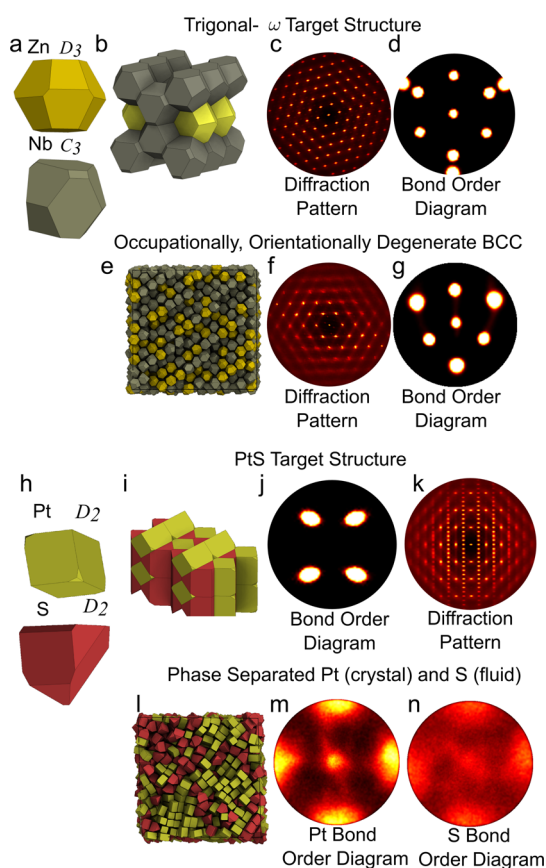
Figure 5. Two examples of assembly in binary VP systems. (a) The two VPs generated by trigonal-ω (ZnNb$_2$) labeled by atom type; (b−d) the target structure; (e−f) the assembled structure, an occupationally degenerate BCC lattice; (h) the two VPs generated by PtS, labeled by atom type; (i−k) the target structure; (l−n) the phase separated, assembly structure.

orientational degeneracy (trigonal-ω) or orientational disorder (β-Mn).

The VPs generated by the PtS crystal (Figure 5h−n) phase separate at $\phi_p = 0.57$, with the VP corresponding to the sulfur atoms crystallizing while the platinum VPs remain fluid. This phase separation is particularly notable because the particles have a densest packing as a cocrystal and thus at some pressure there must be a solid−solid transition from a demixed state to a mixed crystalline state. At low density, these particles are in a mixed fluid state; thus there is a re-entrant mixing transition in this system upon increasing pressure. Any VP mixture exhibiting phase separation also exhibits reentrant mixing behavior.

Assembly Engineering *via* Mesoblock Assembly. Having shown that competing degenerate dense packings may be stabilized relative to space-filling structures away from high pressure, we next modify particle shapes and, through the use of external fields, their assembly pathways so as to disfavor degenerate packings and successfully assemble both the hexagonal diamond target structure examined above, and a carbon 4-ring target crystal structure (Figure 6e).

We consider two general strategies motivated by our findings. In the first strategy, we construct mesoblocks that increase the symmetry of the VPs, thereby reducing the number of degenerate dense packings. When this is insufficient, we consider a second strategy and couple the particle orientations to an external field. A third strategy, not considered here, is to introduce explicit interparticle forces, for example, through the use of attractive ligands, to further disfavor competing packings, as explored for other particle shapes in Khadilkar *et al.*[23] and Millan *et al.*[34]

To illustrate the first strategy, consider the carbon 4-ring crystal structure.[35] The VP of this system has the point group C_{2v}, $IQ = 0.45$ and has two large facet types ($N_{f \geq \mu} = 2$, see Supporting Information, Table SI-2). Because of its low symmetry and expected frustrated bonding between its largest facets (Figure 6), we expect, and confirm, that this particle is a poor assembler—it does not order on the time scale of our simulations. To improve the assembly propensity into the target structure, we construct a two-particle and a four-particle mesoblock. The mesoblock comprising two VPs has C_{2v} symmetry and 2 large facet types—not much improvement over the VP. The mesoblock comprising four VPs is convex and has D_{4h} symmetry and a single large facet type—attributes consistent with particles observed to assemble their space-filling structure (Figure 6g). The latter mesoblock incorporates all particles in the primitive unit cell of the original target structure.

We performed assembly simulations for the VP and the two mesoblocks and found that only the four-VP mesoblock (the most symmetric one of the three shapes) assembles the space filling structure, consistent with our expectations (Figure 6) based on the findings in Figure 2. This observation suggests that to self-assemble some structures, it may be beneficial to incorporate some of the structural complexity into the building block (in this case, four scattering centers) and assemble these higher-symmetry mesoblocks for which there are fewer packing degeneracies.

To illustrate the second strategy, consider again the VP of hexagonal diamond. We constructed a convex mesoblock (D_3) of two HD VPs (C_{3v}), and find that these particles do not assemble any ordered phase. These mesoblocks are identical in shape to the $t = ^2/_3$ particles studied in Haji-Akbari *et al.*[36] In that work, this shape was found to be on the boundary between a fluid region and one that crystallizes into the space-filling structure. However, the crystallization of this particle was reported to be exceptionally difficult, and indeed we were unable to assemble this mesoblock here. The reason assembly is difficult for this shape can be observed by calculations of the PMFT arising from competing local packings or entropically bonded arrangements as pictured in Figure 6c. However, if we disfavor these local packings with the application of an aligning external field (as described in the Methods),
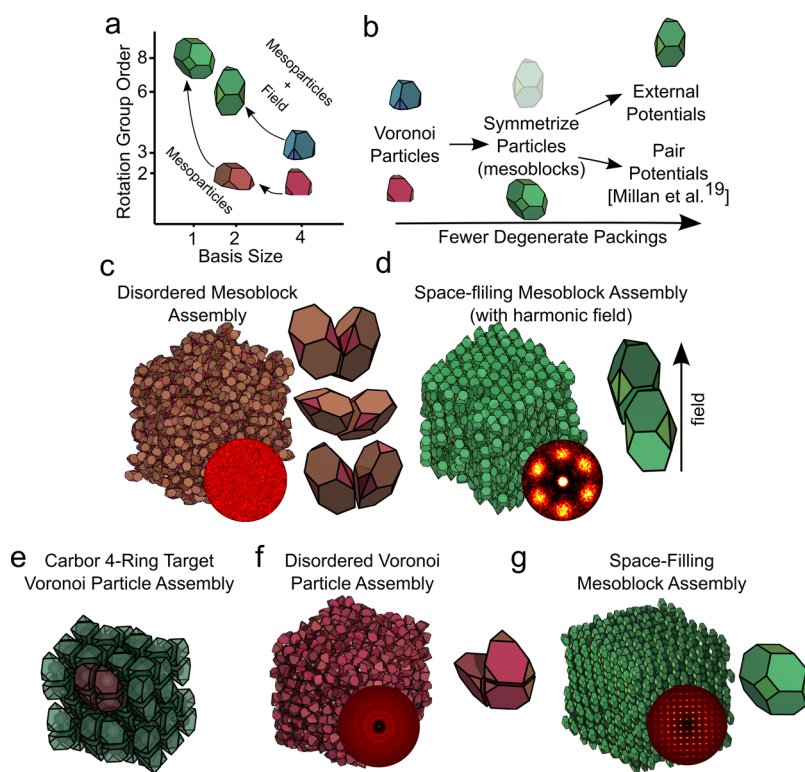
Figure 6. Two examples of engineering hard-particle building blocks using VPs as a basis for design. (a and b) Diagrammatic representations of our particle engineering. (a) A representation of how constructing mesoblocks from VP decreases the size of the effective basis and increases the symmetry of particles. (b) Outline of how these assembly strategies reduce the number of degenerate packings that inhibit assembly of space-filling structures. (c) A first attempt to assemble the hexagonal diamond with a mesoblock. Although this mesoblock increases the symmetry of the basic particle, it also introduces several locally dense packings (shown on the right) that are inconsistent with the crystal structure. (d) An external field is introduced to disfavor these competing packings; this yields the assembly of the target space-filling structures. (e) The Voronoi tessellation of the carbon four-ring structure. The VP does not assemble the target structure (f), but by fusing several VPs together, we can construct mesoblocks of higher symmetry that successfully assemble the target structure (g).

we indeed find its space-filling structure as low as $\phi = 0.56$, shown in Figure 6d. Experimentally, we imagine that such alignment could possibly be achieved *via* shear flow.

DISCUSSION AND CONCLUSION

The role of orientational and occupational packing degeneracies in VP assembly can be understood by considering the contributions to the free energy for such systems. The free energy consists, to first order and ignoring collective effects, of a term from vibrational or rattling motion of the particles and a term from the degeneracy of their local arrangement. Revisiting the relationships between entropy and symmetry, we find that entropy can simultaneously favor symmetry and asymmetry. Globally, entropy favors symmetry; even in orientationally degenerate crystals, the environments of each particle are approximately the same. Vibrational entropy is maximized through the translational symmetry of the lattice. Locally, however, entropy still favors asymmetry. In the single VP systems studied here, local asymmetry takes the form of orientational degeneracies; the system exploits the asymmetry of

the particles to maximize entropy. If particles are sufficiently symmetric, then the system cannot make orientational degenerate configurations that are consistent with the global ordering being driven by thermodynamic assembly. We can further interpret the behavior of many shapes that do not crystallize within this framework; in these cases the entropy of the local, asymmetric packings overwhelms the driving force to maximize vibrational entropy *via* ordering.

Using the Voronoi tessellation, we constructed a set of hard, polyhedral particles (Voronoi particles), whose space-filling configuration is derived from atomic crystals. In the limit of high pressure, the thermodynamic "ground state" of a VP system is guaranteed to be the space-filling structure. At intermediate pressure, we find that although the most symmetric VPs and with uniform faceting assemble their target structure, many VPs assemble nonspace-filling, crystal structures that are stabilized with respect to the target structure by orientational (and, in the multicomponent systems occupational) degeneracies. On the basis of our findings, we have shown examples of how VPs can be modified to enhance selective

entropic bonding and thus assembly. From an engineering standpoint, particles must be designed so that the degeneracy does not destabilize a desired structure.

METHODS

Monte Carlo Simulations of Self-Assembly. We place approximately 2000 hard VPs in a periodic simulation box with disordered initial configuration. The exact number is chosen to be a multiple of the number of particles in the unit cell. Monte Carlo simulations are carried out as described in Haji-Akbari *et al.*[5] over a minimum of 4×10^7 and a maximum of 10^8 Monte Carlo sweeps. For each target structure we conduct *NVT* simulations in a triclinic box commensurate with the target structure at densities $0.53 \leq \phi_p \leq 0.63$ as well as variable box shape *NPT* simulations.

To identify an assembled crystal structure, we compute bond order diagrams and diffraction patterns using the VP centroids and compare them to known crystal structures. The bond order diagram is the histogram of bond orientations projected onto the surface of a sphere. Stereographic projections of the bond orientational diagrams are shown next to simulation snapshots, for example, in Figure 3.

We conduct field-directed self-assembly simulations of the hexagonal diamond VP by placing a director on the 3-fold rotation axis of each particle i, $\hat{n}_i$. An external potential is added to our Monte Carlo simulations of the form $U_{\text{field}} = \sum_{i=0}^{N} \gamma |\hat{n}_i - \hat{z}|^2$, where γ is a spring constant and $\hat{z}$ is the direction of the aligning field. This potential is evaluated with $\gamma = 10$, and trial moves were accepted according to the Metropolis criterion with temperature $T = 1$.

Free Energy Calculations. In select cases, we assess the relative thermodynamic stability of a target, space-filling structure and a competing orientationally degenerate structure by computing the Helmholtz free energies using Frenkel−Ladd thermodynamic integration from a hard particle crystal to an Einstein crystal as described in Haji-Akbari *et al.*[25] In the case of the (orientationally nondegenerate) target structure, Einstein crystal positions and orientations $\{\vec{r}_0, \vec{q}_0\}$ are taken directly from the space-filling tessellation.

Orientationally degenerate crystals have translational order, but each particle can be in one of N_{OD} orientations. For this reason, initializing their coordinates of the Einstein crystal requires additional care. To account for the degeneracy, we assume that the vibrational free energy from translation and rotation is roughly equivalent for each of the orientations and shift the free energy by $-\ln(N_{\text{OD}})k_B T$ per particle. Performing this shift asserts that the system is nonergodic and does not sample all instances of the OD crystal; we have shown this is the case in Figure 4e. Similar shifts have been employed in free energy calculations of degenerate dimer crystals.[26]

To initialize an orientationally degenerate Einstein crystal, we first initialize the simulation at a low density $\phi_p = 0.5$, choose $\{\vec{r}_0\}$ using the target crystal structure, and randomly assign a set of N_{OD}-fold degenerate orientations $\{\vec{q}_0\}$ observed in the assembly. A subsequent compression performing Monte Carlo rotations only allows reaching the desired packing fraction. We verified that our results do not depend on the particular instance of the orientationally degenerate crystal.

Conflict of Interest: The authors declare no competing financial interest.

REFERENCES AND NOTES

1. Macfarlane, R. J.; Thaner, R. V.; Brown, K. A.; Zhang, J.; Lee, B.; Nguyen, S. T.; Mirkin, C. A. Importance of the DNA "Bond" in Programmable Nanoparticle Crystallization. *Proc. Natl. Acad. Sci. U. S. A.* **2014**, *111*, 14995–15000.

2. Zhang, C.; Macfarlane, R. J.; Young, K. L.; Choi, C. H. J.; Hao, L.; Auyeung, E.; Liu, G.; Zhou, X.; Mirkin, C. A. A General Approach to DNA-Programmable Atom Equivalents. *Nat. Mater.* **2013**, *12*, 741–6.

3. Zhang, Y.; Lu, F.; Yager, K. G.; van der Lelie, D.; Gang, O. A General Strategy for the DNA-Mediated Self-Assembly of Functional Nanoparticles into Heterogeneous Systems. *Nat. Nanotechnol.* **2013**, *8*, 865–872.

4. Wang, Z.-G.; Ding, B. DNA-Based Self-Assembly for Functional Nanomaterials. *Adv. Mater. (Weinheim, Ger.)* **2013**, *25*, 3905–3914.

5. Haji-Akbari, A.; Engel, M.; Keys, A. S.; Zheng, X.; Petschek, R. G.; Palffy-Muhoray, P.; Glotzer, S. C. Disordered, Quasicrystalline and Crystalline Phases of Densely Packed Tetrahedra. *Nature (London)* **2009**, *462*, 773–777.

6. Damasceno, P. F.; Engel, M.; Glotzer, S. C. Crystalline Assemblies and Densest Packings of a Family of Truncated Tetrahedra and the Role of Directional Entropic Forces. *ACS Nano* **2011**, *6*, 609–614.

7. Agarwal, U.; Escobedo, F. A. Mesophase Behaviour of Polyhedral Particles. *Nat. Mater.* **2011**, *10*, 230–235.

8. Damasceno, P. F.; Engel, M.; Glotzer, S. C. Predictive Self-Assembly of Polyhedra into Complex Structures. *Science (Washington, DC, U. S.)* **2012**, *337*, 453–457.

9. Qi, W.; de Graaf, J.; Qiao, F.; Marras, S.; Manna, L.; Dijkstra, M. Phase Diagram of Octapod-Shaped Nanocrystals in a Quasi-Two-Dimensional Planar Geometry. *J. Chem. Phys.* **2013**, *138*, 154504.

10. Henzie, J.; Grünwald, M.; Widmer-Cooper, A.; Geissler, P. L.; Yang, P. Self-Assembly of Uniform Polyhedral Silver Nanocrystals into Densest Packings and Exotic Superlattices. *Nat. Mater.* **2012**, *11*, 131–137.

11. Miszta, K.; de Graaf, J.; Bertoni, G.; Dorfs, D.; Brescia, R.; Marras, S.; Ceseracciu, L.; Cingolani, R.; van Roij, R.; Dijkstra, M.; Manna, L. Hierarchical Self-Assembly of Suspended Branched Colloidal Nanocrystals into Superlattice Structures. *Nat. Mater.* **2011**, *10*, 872–876.

12. Young, K. L.; Personick, M. L.; Engel, M.; Damasceno, P. F.; Barnaby, S. N.; Bleher, R.; Li, T.; Glotzer, S. C.; Lee, B.; Mirkin, C. A. A Directional Entropic Force Approach to Assemble Anisotropic Nanoparticles into Superlattices. *Angew. Chem.* **2013**, *52*, 13980–13984.

13. Muller, U. *Symmetry Relationships between Crystal Structures: Applications of Crystallographic Group Theory in Crystal Chemistry (International Union of Crystallography Texts on Crystallography)*; Oxford University Press: USA, 2013; p 360.

14. Meng, G.; Arkus, N.; Brenner, M. P.; Manoharan, V. N. The Free-Energy Landscape of Clusters of Attractive Hard Spheres. *Science (Washington, DC, U. S.)* **2010**, *327*, 560–563.

15. Torquato, S.; Jiao, Y. Dense Packings of the Platonic and Archimedean Solids. *Nature (London)* **2009**, *460*, 876–879.

16. Jain, A.; Errington, J. R.; Truskett, T. M. Inverse Design of Simple Pairwise Interactions with Low-Coordinated 3D Lattice Ground States. *Soft Matter* **2013**, *9*, 3866–3870.

17. Jiao, Y.; Stillinger, F.; Torquato, S. Optimal Packings of Superballs. *Phys. Rev. E: Stat., Nonlinear, Soft Matter Phys.* **2009**, *79*, 041309.

18. Ni, R.; Gantapara, A. P.; de Graaf, J.; van Roij, R.; Dijkstra, M. Phase Diagram of Colloidal Hard Superballs: From Cubes *via* Spheres to Octahedra. *Soft Matter* **2011**, *8*, 8826–8834.

19. Kallus, Y.; Elser, V. Dense-Packing Crystal Structures of Physical Tetrahedra. *Phys. Rev. E: Stat., Nonlinear, Soft Matter Phys.* **2011**, *83*, 036703.

20. de Graaf, J.; van Roij, R.; Dijkstra, M. Dense Regular Packings of Irregular Nonconvex Particles. *Phys. Rev. Lett.* **2011**, *107*, 155501.

21. Chen, E. R.; Klotsa, D.; Engel, M.; Damasceno, P. F.; Glotzer, S. C. Complexity in Surfaces of Densest Packings for Families of Polyhedra. *Phys. Rev. X* **2014**, *4*, 011024.

22. John, B. S.; Juhlin, C.; Escobedo, F. A. Phase Behavior of Colloidal Hard Perfect Tetragonal Parallelepipeds. *J. Chem. Phys.* **2008**, *128*, 044909.

23. Khadilkar, M. R.; Escobedo, F. A. Self-Assembly of Binary Space-Tessellating Compounds. *J. Chem. Phys.* **2012**, *137*, 194907.

24. van Anders, G.; Klotsa, D.; Ahmed, N. K.; Engel, M.; Glotzer, S. C. Understanding Shape Entropy through Local Dense Packing. *Proc. Natl. Acad. Sci. U.S.A.* **2014**, *111*, E4812–E4821.

25. Haji-Akbari, A.; Engel, M.; Glotzer, S. C. Phase Diagram of Hard Tetrahedra. *J. Chem. Phys.* **2011**, *135*, 194101.

26. Marechal, M.; Dijkstra, M. Stability of Orientationally Disordered Crystal Structures of Colloidal Hard Dumbbells. *Phys. Rev. E: Stat., Nonlinear, Soft Matter Phys.* **2008**, *77*, 061405.

27. Center for Computational Materials Science of the United States Naval Research Laboratory. Crystal Lattice Structures Web page. 04−02−2012; http://cst-www.nrl.navy.mil/lattice/.

28. Rice, R.; Roth, R.; Royall, C. P. Polyhedral Colloidal 'Rocks': Low-Dimensional Networks. *Soft Matter* **2012**, *8*, 1163–1167.

29. van Anders, G.; Ahmed, N. K.; Smith, R.; Engel, M.; Glotzer, S. C. Entropically Patchy Particles: Engineering Valence through Shape Entropy. *ACS Nano* **2014**, *8*, 931–940.

30. Haji-Akbari, A.; Engel, M.; Glotzer, S. C. Degenerate Quasicrystal of Hard Triangular Bipyramids. *Phys. Rev. Lett.* **2011**, *107*, 215702.

31. Schofield, A. Binary Hard-Sphere Crystals with the Cesium Chloride Structure. *Phys. Rev. E: Stat., Nonlinear, Soft Matter* **2001**, *64*, 051403.

32. Bartlett, P.; Ottewill, R.; Pusey, P. Superlattice Formation in Binary Mixtures of Hard-Sphere Colloids. *Phys. Rev. Lett.* **1992**, *68*, 3801–3804.

33. Khadilkar, M.; Agarwal, U.; Escobedo, F. Phase Behavior of Binary Mixtures of Convex Hard Polyhedra. *Soft Matter* **2013**, *9*, 11557–11567.

34. Millan, J. A.; Ortiz, D.; van Anders, G.; Glotzer, S. C. Self-Assembly of Archimedean Tilings with Enthalpically and Entropically Patchy Polygons. *ACS Nano* **2014**, *8*, 2918–2928.

35. Schultz, P.; Leung, K.; Stechel, E. Small Rings and Amorphous Tetrahedral Carbon. *Phys. Rev. B: Condens. Matter Mater. Phys.* **1999**, *59*, 733–741.

36. Haji-Akbari, A.; Chen, E. R.; Engel, M.; Glotzer, S. C. Packing and Self-Assembly of Truncated Triangular Bipyramids. *Phys. Rev. E: Stat., Nonlinear, Soft Matter* **2013**, *88*, 012127.